17th World Conference on Earthquake Engineering, 17WCEE
Sendai, Japan - September 13th to 18th 2020

RESPONSE OF THE TALLEST CALIFORNIA BUILDING DURING THE Mw7.1 JULY 5, 2019 RIDGECREST, CALIFORNIA EARTHQUAKE

M. Çelebi[(1)], S.F. Ghahari[(2)], H. Haddadi[(3)], E. Taciroglu[(2)]

(1) Senior Research Civil Engineer, U.S. Geological Survey, Earthquake Science Center, Menlo Park, California. celebi@usgs.gov
(2) Department of Civil Engineering, University of California, Los Angeles, California
(3) Manager, StrongMotion Instrumentation Program, California Gelogical Survey, Sacramento, California

Abstract

The 73-story Wilshire Grand in downtown Los Angeles is the recently constructed tallest building in California. It is designed in conformance with performance-based design procedures. The lateral load resisting system of the building is designed with concrete core shear walls, three outriggers with buckling restrained braces (BRBs) located along the height and two three-story truss-belt structural systems. The building is equipped with a 36-channel accelerometric seismic monitoring array that recorded the recent Mw7.1 Ridgecrest earthquake of July 5, 2019, as well as the Mw6.4 July 4, 2019 Ridgecrest Earthquake. In this paper, only the Mw7.1 July 5, 2019 event is studied because of a larger response of the subject building during that earthquake. The earthquake records of July 5, 2019 are specifically studied to determine its dynamic characteristics and building specific behavior. The structure exhibits torsional behavior most likely due to abrupt asymmetrical changes in the thickness and size in-plan of the core shear wall system. Modal shapes, frequencies and critical damping percentages of the building are identified. The translational and torsional modes during the earthquake are not closely coupled with fundamental NS, EW and torsional frequencies (periods) of 0.16 (6.25), 0.27(3.70) and 0.42 (2.38) Hz (seconds). This does not lead to a beating effect even though there is an appearance of it in the displacement records. Due to the relatively low amplitude of shaking during the earthquake, the drift ratios are too small to cause any damage. It is expected that during stronger shaking levels likely to be caused by future events, these characteristics may change and the effect of BRB's can be better assessed.

Keywords: earthquake response, mode shape, frequency, damping, drift ratio

1. Introduction

The number of tall buildings in the United States and around the world is increasing with an awe-inspiring race for height. While displaying novel architectural features and structural innovations, tall buildings pose challenges to structural engineering design, analyses, and construction materials and construction techniques. Their designs are also expected to provide (and be scrutinized to assure) requisite dynamic behavior and performances during extreme events, such as strong winds or shaking caused by earthquakes that originate from near and far seismic sources. The designs must also comply with updated and redefined new and older seismic hazards, associated risks to the built environment, and acceptable performance criteria. The introduction of new construction materials, high-strength concrete, and steel, as well as structural response modification features, generate new opportunities for enhanced performance-based design as well. While the behavior and performances of tall buildings can be assessed by computations and visual inspections, more and more, data-based evaluations are being considered to satisfy the needs of owners and other stakeholders. However, it is fair to state that the number of instrumentally monitored tall buildings to yield response data during strong-shaking events is very limited (e.g. less than 1% of tall buildings are being monitored). It is

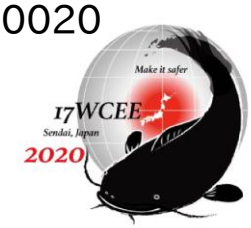

therefore an important attribute that one of the new additions to the panorama of Los Angeles, California – the 73-story Wilshire Grand (hereafter referred to as The Building) - with its spire at the top, is not only the current tallest (~335 m [~1098 ft]) building in downtown Los Angeles and the State of California but it is also instrumented (by the California Strong Motion Instrumentation Program [CSMIP] of the State of California Geological Survey [CGS] as Station #24660). Thus, it fulfills a need and facilitates a real-life behavior and performance study of this unique building – which we describe in this paper.

The building is designed to have a concrete shear wall core with dynamic response modification features - a type of design and construction that is not new, but recently has been used more often with taller buildings. Thus, the building offers the opportunity to study the response of such a tall building to seismic (and, when needed, ambient) shaking as well as strong winds. Such an opportunity now exists with the recorded responses of the building during the M7.1 July 5, 2019 Ridgecrest earthquake [7.1Mw, 20:19:53 PDT, 35.7695N 117.5993W Depth 8.0 km] that occurred at an epicentral distance of ~200km from the building (www.strongmotioncenter.org, last accessed September 30, 2019). This study is the first in-depth study of the behavior and performance of Wilshire Grand during an earthquake. To date, the authors are not aware of any similar study of this building. Although responses of the building during another Ridgecrest earthquake (Mw6.4) were also recorded on July 4, 2019, at about similar epicentral distance from the Building, we chose to use the larger accelerations from the M7.1 mainshock as summarized in Table 1. Ambient shaking is also much smaller in amplitude compared to either earthquake; hence, it is not included within the scope of this paper.

Table 1. Particulars of the two Ridgecrest Earthquakes (*from* www.strongmotioncenter.org, last accessed September 30, 2019)

Date	M_w	Epicentral Distance (km)	Earthquake Origin Time (UTC)	Peak Accel. (g)	
				Ground	Building
July 4, 2019	6.4	196.1	2019-07-04 17:33:49	0.011	0.073
July 5, 2019	7.1	199.7	2019-07-06 03:19:53	0.016	0.095

Thanks to seismic structural monitoring projects, long-distance / long-period responses of tall buildings severely shaken by events that occur at far distances has been the subject matter of many recent studies [1-7].

2. Building Structural System, Foundation, and Site

2.1. Structural system

The building is 73 stories above and 5 stories of parking levels below ground level. The base dimensions of the building are 124.4m x 103.3m (408 ft x 339 ft). The tower structure starts with an approximately 66.7m x 27.9m (218.75ft x 92.4ft) at the ground level and tapers off to approximately 46.2m x 29.2 m (151.8ft x 95.8ft) at the 73rd level. A picture and vertical sections of the building are provided in Fig. 1. Arrows and dots in the vertical sections display the levels and orientations of the accelerometers. The monitoring array is described later in the paper.

The lateral load-carrying system comprises the core shear wall (4 feet thick at the base tapering to 2 feet at the top), three outriggers and two truss-belt structural systems. (Fig. 1). In the transverse direction, the outriggers with buckling restrained braces (BRBs) are placed at three locations along the height of the structure (Levels 28 to 31, Levels 53 to 59, and Levels 70 to 73). Two three-story tall belt trusses are around the perimeter at the lower and upper outrigger levels (www.strongmotioncenter.org, last accessed September 30, 2019). Twenty columns that work with the outriggers are built of concrete-filled steel boxes.

Fig. 2 displays dimensions of the concrete core shear walls that start with 1.22m (4 ft) thickness at P5 level to 28_{th} level, 0.91m (3 ft) between the 28_{th} and 41_{st} levels, and 0.61m (2 ft) between the 41_{st} and 73_{rd}

levels. Between the 73rd and 75th levels, there is a 16.9 (55.4ft) (tall) steel structure (Figs - 1 and 2). Ratios of shear wall area to floor area have been computed to be at a minimum of 4.0% [8].

As an approximation, the relative core shear wall areas and floor areas and percentages are summarized in Table 2. Thus, with a minimum ~ 4 % core/shear wall ratio, this building has a comparable (or higher) shear wall area percentage when compared with the practice in Chile where core shear walls are widely applied in design and construction [9-11] Such buildings performed well during the 1985 Valparaiso (Mw7.8) [12] and 2010 Maule (Mw8.8) earthquakes in Chile.

The vertical load varrying system comprises:

1. concrete beams and slabs inside the core walls (outside the core walls, lightweight concrete over metal deck supported by (a) steel beams, (b) perimeter steel box columns filled with concrete).
2. concrete core walls and concrete flat slabs at the first floor and below.
3. at the top of the building, a glazed steel braced frame structure (sail) standing 29.6 m (97 ft) above the main roof at level 73. The 90.0 m [295 ft] long tubular steel cantilever spire extends above the roof.
4. a low-rise podium is adjacent to the Lateral Force Resisting System Concrete core shear walls (1.22 m [4 ft] thick at the base tapering to 0.61 m [2 ft] at the top) with outriggers and belt trusses.
5. in the transverse direction, the outriggers with buckling restrained braces (BRBs) are placed at three locations along the height of the structure (Levels 28 to 31, Levels 53 to 59, and Levels 70 to 73). Two three-story tall belt trusses are around the perimeter at the lower and upper outrigger levels (www.strongmotioncenter.org, last accessed September 30, 2019).

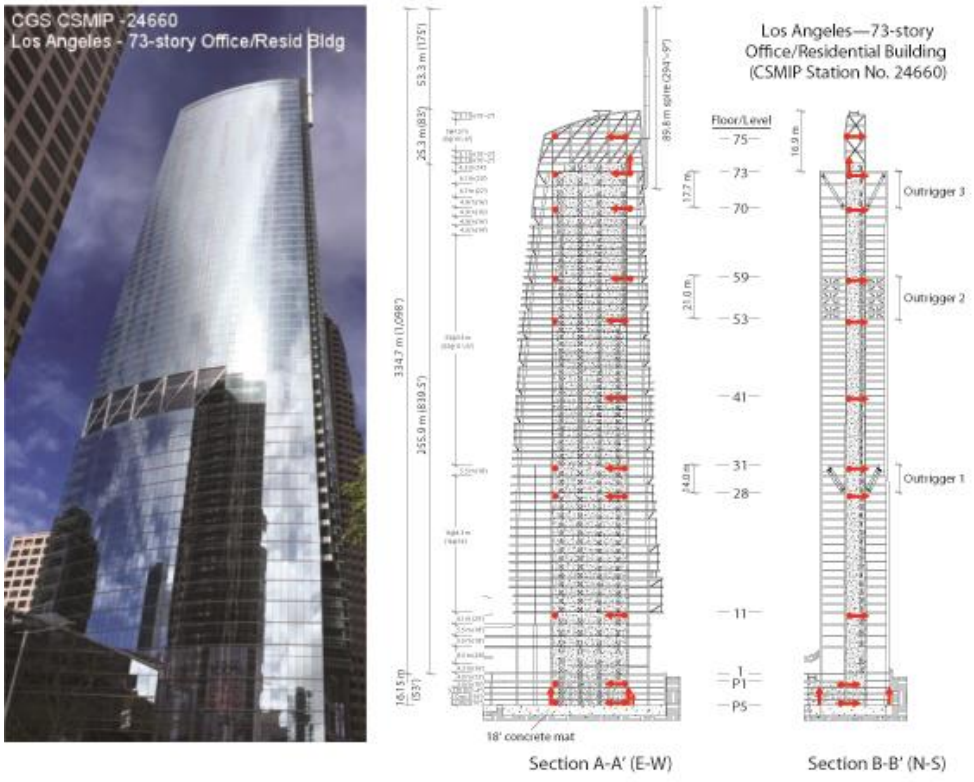

Fig. - 1. Photo of the building and N-S and E-W vertical sections. Vertical sections of the building depict vertical dimensions, the locations of outriggers and belt trusses as well as the levels at which accelerometers are deployed (arrows indicate orientations). Photo is cropped and sections are modified from www.strongmotioncenter.org, last accessed September 30, 2019).

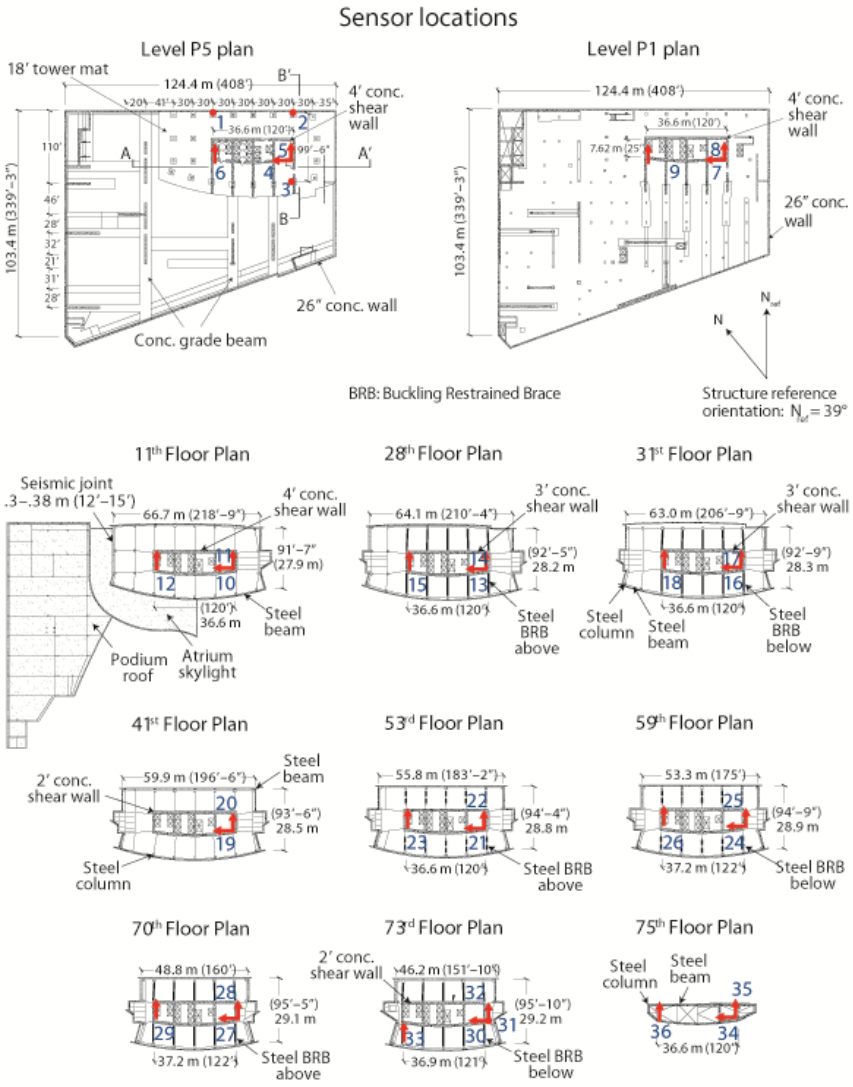

Fig. - 2. Plan-views of floors showing the core-shear walls and deployed accelerometers with locations and orientations. Figure modified from www.strongmotioncenter.org (last accessed September 4, 2019).

2.2. Building design criteria

The structural design of the building is based on performance-based seismic design and the 2011 City of LA Building Code (2010 CBC) (www.strongmotioncenter.org, last accessed September 4, 2019). The Performance-Based Earthquake Engineering (PBEE) procedures include nonlinear dynamic analyses using site-specific design response spectra for serviceability (or service level design earthquake [SLDE]) when ground motions with 50% probability of exceedance in 30 years) and low probability of collapse when ground motions with 2% probability of exceedance in 50 years and is defined as an extremely rare event or Maximum Considered Earthquake (MCE) [in accordance with the Los Angeles Tall Buildings Seismic Design Council (LATBSDC, 2011] recommendations [13]. This has been done by computing (a) probabilistic MCE response spectrum (with a 2% probability of being exceeded in 50 years), and (b) deterministic MCE response spectrum as the maximum of the composite deterministic response spectrum and the deterministic lower limit as defined on Figure 21.2-1 of American Society of Civil Engineers 7-05

Standard (ASCE, 2005)[14]. Then, the site- specific MCE response spectrum has been adopted as a composite of the lesser of the ordinates of the probabilistic and deterministic MCE response spectra [15]. A plot of the resulting site-specific MCE and SLDE response spectra are provided in Fig. 3. For further details of the development of probabilistic and deterministic design response spectra, the reader is referred to the [15].

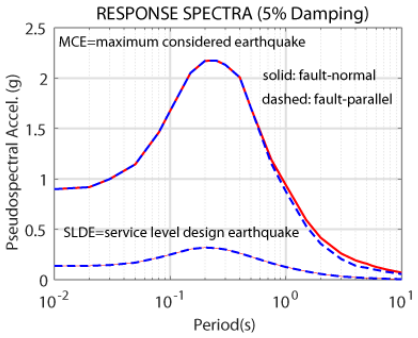

Fig. - 3. Design response spectra (5% damped) for maximum considered (MCE) and service level design earthquake (SLDE) (replotted with spectra data source from [15]).

2.3. Site and foundation

The Building is supported on a 5.49m (18 ft) thick concrete mat foundation. The foundation is supported on bedrock (www.strongmotioncenter.org, last accessed September 4, 2019, and [15]).

For the building site, CTL (a general description of site geology) is given as shallow alluvium over sedimentary rock. The site class is described as C for which a measured Vs30 is given as 500 m/s (www.strongmotioncenter.org, last accessed September 16, 2019). Using Vs30, an approximate computation yields a site period (T_s) ~4x30/500 ~ 0.24 seconds. Based on this approximation for CTL only, it may be interpreted that there would be no site effects on a 73-story building (Wilshire Grand) with a pre-estimated building period (T_b) ~5-7 seconds. More accurate computations for the site period (T_s) using borehole logs of CTL would certainly yield approximate Ts<1 second.

However, in Los Angeles, when geotechnical and geological settings are discussed, usually, in addition to "geotechnical layer" (CTL) considered mostly for low-rise buildings, basin geology and deep velocity structure is also taken into account for tall buildings in consideration of long-distance long-period effects of motions generated by sources at far distances. Long-distance is normally interpreted as > fault rupture length [16]. Such basin effects have been observed and studied before (e.g. effect of Mw9.0 Tohoku earthquake of 2011 on the response of a 55-story building in Osaka at ~770 km from the epicenter [1,5], and in Tokyo at 375 km from the epicenter [17]. In addition, an earlier study of earthquake responses of a 58-story building a few blocks away from the Wilshire Grand in downtown Los Angeles also yielded low site frequency (long period) ~0.12-0.13 Hz (7.7-8.3s) [3]. These are included herein primarily to draw attention to the basin effect so that future studies of existing and future long-period structures in that area can make use of such similarity and consider basin effects in assessing site effects. Therefore, the implication is that it is likely that the impact of the deeper geological structure may affect the dynamic response of this (or any other) tall building (greater than ~ 40-50 stories).

Therefore, it is deemed important that in consideration of deep velocity structures in the Los Angeles basin, where Wilshire Grand is, we draw attention to the possible effect of the basin on the specific site. Hence, in this study, velocity profiles generated by Graves [18] are used to compute site transfer functions to estimate site frequencies due to the deep velocity structure. Two profiles have been computed using community velocity models, cvms and cvmh [18] described in detail in [8]. The site transfer functions computed using the two community velocity model profiles are shown in Fig. 4 with estimated fundamental site frequencies (periods) between 0.11-0.16Hz (6.3-9.1s) – well within range of fundamental frequency of a 73-story building.

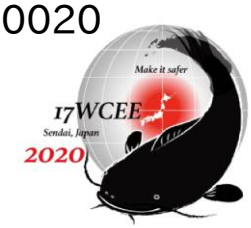

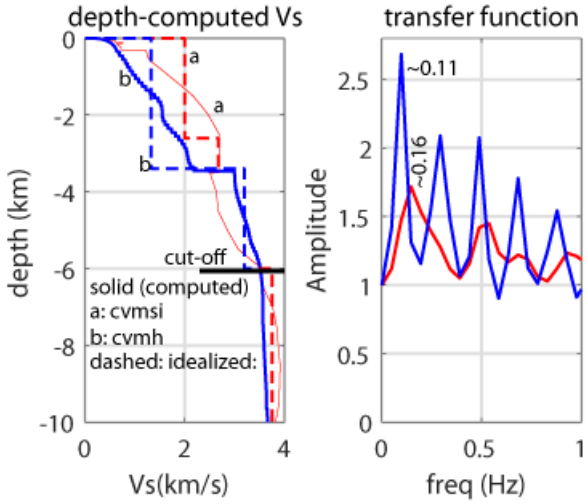

Fig. - 4. (i) Vs-depth profiles in solid and approximated dash lines for community velocity models (CVM) (a) red [CVM-S] and (b) blue [CVM-S] for Wilshire Grand site (CSMIP station 24660) in downtown Los Angeles. Alternate variations of approximations of step profiles should not alter the results significantly. Thus, the results are representative of other tall buildings in the immediate vicinity of Wilshire Grand. (ii) Transfer function is computed for approximated (dashed) step profiles a and b.

2.4. Seismic monitoring array and distribution

Seismic instrumentation of the building was completed by CSMIP in 2017, with 36 accelerometers deployed at 11 levels (www.strongmotioncenter.org, last accessed September 4, 2019). The seismic monitoring array of the building is depicted in vertical sections and plan views presented in Figs. 1 and 2. For ease in following the analyses in this study (or future studies), the 32-channels of data sets are organized in Table 2 according to the location (height of the level of each channel sensor and orientation).

Table 2. Distribution and number labeling of channels according to orientations and along the height (and floor level) of the building.

Floor/ Level	Height between P5 upwards)		Between instrumented levels		NS1 (left)	NS2 (right)	EW	VERT
	H(ft)	H(m)	Between Levels/Floors	H(m)				
Level P5	0	0	0		6	5	4	1,2,3
Level P1	40	12.19	P1 andP5	12.19	9	8	7	
1	53	16.15						
11	153	46.63	11 and P1	34.44	12	11	10	
28	349	106.37	28 and 11	59.74	15	14	13	
31	395	117.35	31 and 28	10.98	18	17	16	
41	510	155.45	41 and 31	38.10		20	19	
53	648	197.51	53 and 41	42.06	23	22	21	
59	717	218.54	59 and 41	21.03	26	25	24	
70	832	253.59	70 and 59	35.05	29	28	27	
73	890	271.27	73 and 70	17.68	33	32	30	31
75	945.33	288.14	75 and 73	16.87	36	35	34	

3. Earthquke Data and Analyses

3.1. Acceleration and displacement time histories, and drift ratios

Fig. 5 shows horizontal NS, EW, and torsional acceleration time histories. “Torsional” is defined as the difference between two NS channels (NS1 and NS2) on one instrumented floor. There is only one accelerometer in the NS direction on 41st floor; hence, no torsional acceleration is computed or plotted at that level. Note also that, in addition to three vertical channels (CH1, CH2, and CH3) at the P1 level, there is an additional vertical channel (CH31) at the 75th level. The vertical acceleration data from these channels are used to assess rocking around NS and EW axes if any, of the building, as discussed later in the paper.

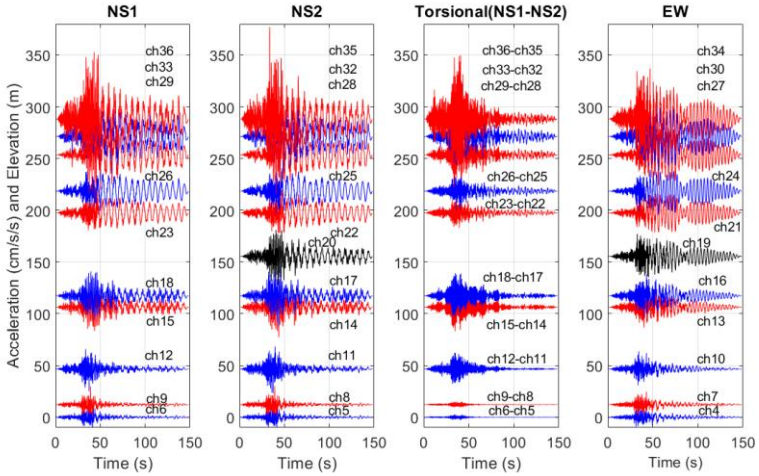

Fig. -5. Equiscaled acceleration time-histories of horizontal channels plotted against the elevation of the channels at a particular level and corresponding height of the building and according to line-up summarized in Table 3. Note the vertical axis is used for both the amplitude of acceleration (in cm/s^2) and elevation (in meters).

Similarly, Fig. 6 shows the corresponding displacement time-histories. What is noted in the time histories are (a) after 50 seconds into the records, it appears that the building vibrations are in fundamental period in their respective directions, and (b) apparent beating response is clearly observed in the EW direction displacements.

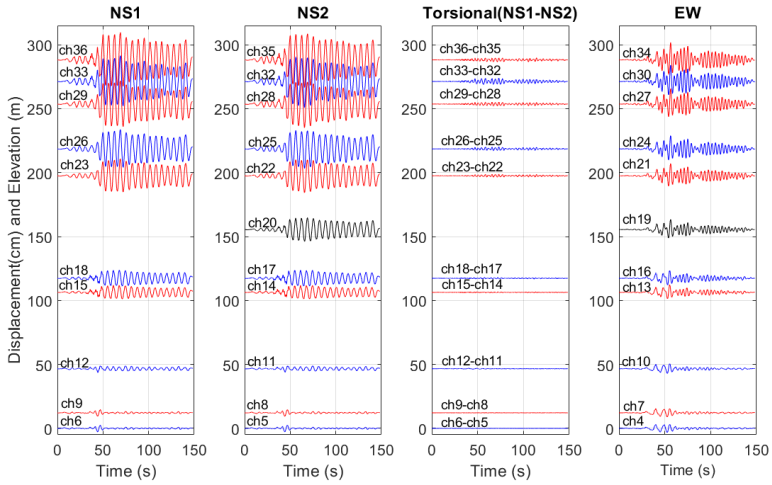

Fig. - 6. Equiscaled displacement time-histories of horizontal channels plotted against the elevation of the channels at a particular level and corresponding height of the building and summarized in Table 3. Note the vertical axis is used for both the amplitude of displacement (in cm) and elevation (in meters).

Even though damaging shaking during the July 5, 2019 earthquake did not occur, as a routine check, it is useful to quantify average drift ratios, as one of the parameters that can be extracted from the records to informedly state that there was no damage during the event.

In Fig. 7a and b, average drift ratios computed between two consecutive instrumented levels in descending order from top to bottom for the NS2 and the EW directions, respectively are presented. This is an informative display of the stability of average drift ratios between consecutive instrumented levels. The largest average drift ratios in the NS2 and EW directions are ~ 0.11% and 0.06%, respectively. These drift ratios are too small to cause any damage. In addition, it is essential to state that the time-histories of drift ratios do not exhibit any unusual variation due to the presence of three-stories each of the three outriggers between the 28th and 31st, 53rd and 59th, and 70th and 73rd levels.

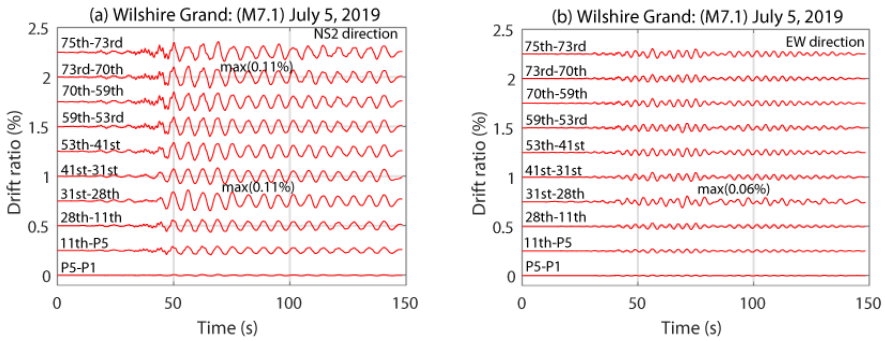

Fig. - 7. (a) Computed average drift ratios between two consecutive instrumented levels in descending order from top to bottom. (a) for the NS2 direction and (b) for the EW direction. Note that the largest average drift ratios ratios in the NS2 and EW directions are ~ 0.11% and 0.06%, respectively.

3.2. Spectral ratios of amplitude spectra

Fig. -8 shows the spectral ratios (of amplitude spectra – not shown herin) between various levels with respect to P5. Note that these plots are smoothed in the frequency domain by convolving spectra with a Hanning window. The dominant peaks in these plots denote the natural frequency of the superstructure in which additional flexibility through soil-foundation rocking interaction is included (pseudo-flexible base system [22]).

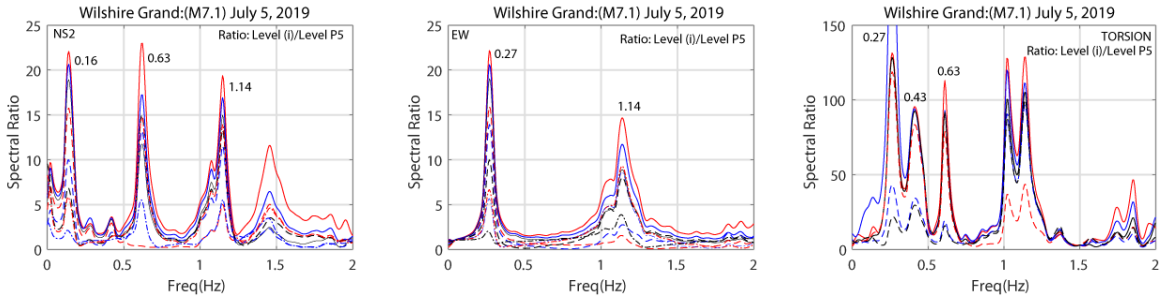

Fig. - 8. Spectral ratios of smoothed amplitude spectra of accelerations at a particular level in one direction (from top in descending order) with respect to that at P5 level in the same direction reveal the structural frequencies including possible soil-foundation rocking flexibility.

3.3. Foundation rocking

The presence of three vertical channels (CH1, CH2 and CH3) at the basement (Level P5) allows computation of basement rotation around NS and EW axes. In Fig. 9, amplitude spectra of relative rocking (or rotational) accelerations of the vertical channels CH1-CH2 (around the NS axis) and CH2-CH3 (around the EW axis)

are shown. Again, both spectra clearly contain the fundamental frequencies in the NS (0.16 Hz) and EW (0.27Hz) directions, respectively. These imply that there is soil-structure interaction in the form of rocking at the basement.

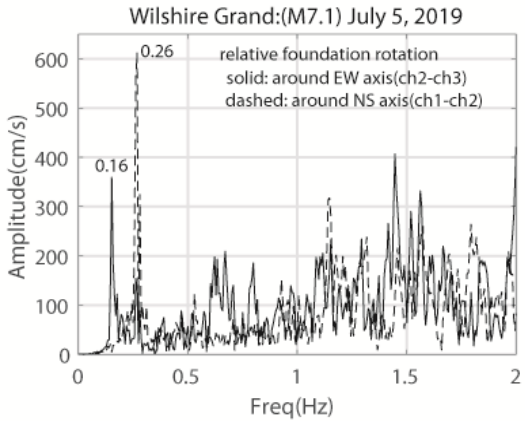

Fig. - 9. Amplitude spectrum of relative rotational accelerations (CH1-CH2) around the NS axis and (CH2-CH3) around the EW axis**.** Translational fundamental frequencies NS (0.16Hz) and EW (0.26Hz) appear in the spectra and imply rocking of the basement (basemat in this case).

3.4. System identification

Input-output (Subspace State-Space) System Identification (4SID) was performed to identify fundamental modal properties (natural frequencies, damping ratios, and mode shapes) [23,24]. The recorded accelerations at the Level P5 are used as input signals, while recorded signals at instrumented floors are used as output signals. As the number of signals and their length are quite large, we reduce the complexity of the problem by using following simplifications:

- The signals are low-pass filtered to remove frequencies above 4 Hz. Otherwise, a very large model order would be needed to be able to identify a few fundamental modes due to the contribution of the higher and local modes.
- There are two NS-oriented sensors on each floor, so it is possible to theoretically remove the torsional effects and decouple NS from two degrees of freedoms (DOF's). Hence, we use the average of these signals as representative of NS response and split the identification into two separate problems: NS and EW-Torsion directions.
- There is only one NS channel on the 41st floor. We used the average of torsional responses of floors 31 and 53 to calculate torsional response of the floor 41st. Then, we used this torsional acceleration and estimated NS response in the west side and consequently calculated average NS response.

It is noteworthy to mention again that the modal properties identified here are pseudo-flexible properties [22], as foundation rocking was not considered as part of the input signals. The first three natural frequencies and corresponding critical damping percentages are inserted in each of the NS, EW and torsional mode shape plots in the summary Fig. 10 as well as in Table 3 at the end of the paper. Note that the critical damping percentages are lower tan the usual 5% critical damping ratio used in the design process but is consistent with the latest recommendations of LATBSDC [13].

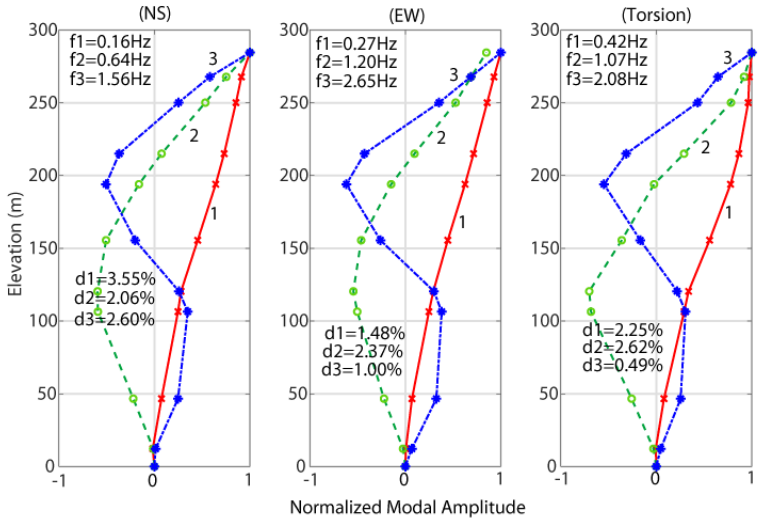

Fig. - 10. First three mode shapes of the building in NS, EW, and Torsional directions each depicting the first three fundamental frequencies and critical damping percentages.

4. Discussion of Results and Conclusions

The analyses presented in this paper covers the dynamic behavioral characteristics due to the recorded responses of the building to the largest shaking experienced by the building to date; and yet, given the seismic hazard due to many seismic zones in Los Angeles and vicinity, it is not the strongest shaking it may experience in the future. Therefore, based on this earthquake data, with a maximum of average drift ratio of 0.11%, as expected, there is no damage to the building. As a result of system identification and spectral analyses including spectral ratios, we confirm that the first three modal frequencies (periods) and critical damping percentages are as in Table 3. Furthermore, we note that, although it was out of the scope of this paper, available ambient data analyses indicated that for the first mode, the frequency (by system identification) is identical to that of the earthquake data-based. This means there is likely no significant nonlinearity in the soil or structure.

Table 3. Natural frequency (period) and modal damping ratios identified using system identification method.

	Frequency (Hz)/Period (s)			**Damping ratio (%)**		
Dir.\Mode	1	2	3	1	2	3
NS	0.16/6.25	0.64/1.56	1.56/0.64	3.55	2.06	2.60
EW	0.27/3.70	1.20/0.83	2.65/0.38	1.48	2.37	1.00
Torsion	0.42/2.38	1.07/0.93	2.08/0.48	2.25	2.62	0.49

No particular tendency is evident between damping ratios extracted from the earthquake and ambient data. Although no computation is offered a beating effect is observable particularly in the EW displacement plots in Fig. 6.

5. Data Source: www.strongmotioncenter.org, last accessed December 12, 2019

6. Acknowledgments: The authors thank Robert Graves of U.S. Geological Survey for generating Depth - V_s profiles for the site of this building.

7. References

[1] Çelebi, M., Okawa, I., Kashima, T., Koyama, S. and M. Iiba, M. (2014): Response of a tall building far from the epicenter of the March 11, 2011 M=9.0 Great East Japan earthquake and its aftershocks, The Wiley Journal of The Structural Design of Tall and Special Buildings. and in volume: 23, 427-441. doi:10.1002/tal.1047

[2] Çelebi, M., Hisada, Y., Omrani, R., Ghahari, F., and Taciroğlu, E. (2016a): Responses of two tall buildings in Tokyo, Japan, before, during, and after the M9.0 Tohoku Earthquake of March 11, 2011., *Earthquake Spectra,* February 2016, Vol. 32, No. 1, pp. 463-495.

[3] Çelebi, M., Ulusoy, H., and Nakata, N. (2016b): Responses of a tall building in Los Angeles, California as inferred from local and distant earthquakes, *Earthquake Spectra*, v32, no 3, pp 1821-1843. doi: 10.1193/050515EQS065M.

[4] Çelebi, M., Kashima, T., Ghahari, S. F., Koyama, S., and Taciroğlu, E. (2017): Before and after retrofit dynamic characteristics of a 55-story building, PROC. EVACES2017 [Experimental Vibration Analysis for Civil Engineering Structures, July 12-14, 2017, UC San Diego, La Jolla, California.

[5] Çelebi, M., Kashima, T., Ghahari, S.F., Koyama, S., Taciroğlu, E., and Okawa, I. (2018). Dynamic Characteristics of a 55-Story Building Before and After Retrofit, Springer International Publishing AG 2018 J.P. ***in*** Conte et al. (eds.), Experimental Vibration Analysis for Civil Structures, Lecture Notes in Civil Engineering 5, pp. 656-666, doi:10.1007/978-3-319-67443-8_57.

[6] Skolnik D., Ciudad R.M., Franke M., Milutinovic D.Z., Ahmed A., Ali M., Kaya Y., and Safak E. (2013): Operation of the structural health monitoring network of unique structures in Abu Dhabi Emirate, 8th Gulf Seismic Forum, 3–6 March. Oman, Muscat.

[7] Safak, E. Kaya, Y., Skolnik, D., Ciudad-Real, M., Al Mulla, H., and Megahed, A. (2014): Recorded response of a tall building in Abu Dhabi from a distant large earthquake, May 2014: Proc. 10th U.S. National Conference on Earthquake Engineering. doi: 10.4231/D3C53F215.

[8] Çelebi, M., Ghahari, S.F., Haddadi, H., and Taciroglu, E. (2019): Response Study of the Tallest California Building Inferred from the Mw7.1 July 5, 2019 Ridgecrest, California Earthquake and Ambient Motions, *in print*, ***Earthquake Spectra.***

[9] ICH. (2002): *Edificio chilenos de Hormigon Armado*, ICH Instituto del Cemento y del Hormigon de Chile, 2002.

[10] Lagos, R. (2010): Personal oral communication.

[11] Lagos, R., Kupfer, M., Lindenberg, J., Bonelli, P., Saragoni, R., Guendelman, T., Massone, L., Boroschek, R., and Yañez, F. (2012): Seismic Performance of High-Rise Concrete Buildings in Chile, *International Journal of High-Rise Buildings*, 1, 3, 181-194.

[12] Çelebi, M., and Sembera, E. (1985): Preliminary evaluation of performance of structures, in *Preliminary Report of Investigations of the Central Chile Earthquake of March 3, 1985, (ed. S. T. Algermissen),* U.S. Geological Survey Open-FileReport 85-542, doi:10.3133/ofr85542. (http://pdf.usaid.gov/pdf_docs/PNABF571.pdf).

[13] LATBSDC (2017): Los Angeles Tall Buildings Structural Design Council, *An alternative procedure for seismic analyses and design of tall buildings located in the Los Angeles region: A consensus document.* 72pp.

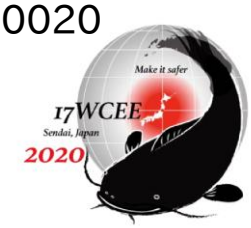

[14] ASCE (American Society of Civil Engineers), (2005): ASCE/SEI Standard 7-05: Minimum Design Loads for Buildings and Other Structures. American Society of Civil Engineers.

[15] AMEC (2012): Report of Geotechnical Consultation Proposed Wilshire Grand Project, 930 West Wilshire Boulevard, Los Angeles, California (non-public report)

[16] Boore, D. (2015): written communication.

[17] Çelebi, M., Kashima, T., Ghahari, S. F., Abazarsa, F., Taciroglu, E. (*2016*): Responses of a Tall Building with U.S. Code-Type Instrumentation in Tokyo, Japan, to Events Before, During, and After the Tohoku Earthquake of 11 March 2011. *Earthquake Spectra*: Vol. 32, No. 1, pp. 497-522, February 2016,

[18] Graves, R., (2019): written communication. April 1, 2019.

[19] Boroschek, R. L., and Mahin, S. A. (1991): Investigation of the seismic response of a lightly-damped torsionally-coupled building: Univ. of California, Berkeley, Earthquake Engineering Research Center Report UCB/EERC-91/18, 291pp.

[20] Çelebi, M. (2006): Recorded earthquake responses from the integrated seismic monitoring network of the Atwood Building, Anchorage, (Alaska), *Earthquake Spectra*, 22:4, 847-864, November 2006.

[21] Çelebi, M.(2018): Quantifying the effect of beating inferred from recorded responses of tall buildings, *Proceedings of 16th European Conference on Earthquake Engineering*, Thessaloniki, Greece, 18-21 June 2018, 12 pp. PROC. 16ECEE, Thessaloniki, Greece, June 18-21, 2018.

[22] Stewart, J. P., and Fenves, G. (1998). System identification for evaluating soil–structure interaction effects in buildings from strong motion recordings. *Earthquake Engineering & Structural Dynamics*. 27, 8 (1998): 869-885.

[23] Van Overschee, P. and De Moor, B. (1994, N4SID): Subspace algorithms for the identification of combined deterministic-stochastic systems. *Automatica* 30.1, pp. 75-93.

[24] Van Overschee, P. and De Moor, B. (1996): *Subspace identification for linear systems*. Kluwer Academic Publishers, Dordrecht, The Netherlands.

